

9-1-2010

The Effect of Boron-Containing Layered Hydroxy Salt (LHS) on the Thermal Stability and Degradation Kinetics of Poly (Methyl Methacrylate)

Stephen Majoni
Marquette University

Shengpei Su
Hunan Normal University

Jeanne Hossenlopp
Marquette University, jeanne.hossenlopp@marquette.edu

Accepted version. *Polymer Degradation and Stability*, Vol. 95, No. 9 (September 2010): 1593-1604.
DOI. © 2010 Elsevier. Used with permission.

NOTICE: this is the author's version of a work that was accepted for publication in *Polymer Degradation and Stability*. Changes resulting from the publishing process, such as peer review, editing, corrections, structural formatting, and other quality control mechanisms may not be reflected in this document. Changes may have been made to this work since it was submitted for publication. A definitive version was subsequently published in *Polymer Degradation and Stability*, VOL 95, ISSUE 9, September 2010, DOI.

The Effect of Boron-Containing Layered Metal Hydroxy Salt (LHS) on the Thermal Stability and Degradation Mechanisms of Poly(Methyl Methacrylate)

Stephen Majoni

*Department of Chemistry, Marquette University
Milwaukee, WI*

Shengpei Su

*Department of Chemistry and Chemical Engineering, Hunan
Normal University
Changsha, China*

Jeanne M. Hossenlopp

*Department of Chemistry, Marquette University
Milwaukee, WI*

Abstract:

A boron-containing layered hydroxy salt (LHS), ZHTMDBB, was prepared and compounded with a highly flammable synthetic polymer, poly (methyl methacrylate) {PMMA}, via melt blending: the composite structure was intercalated with poor dispersion. The effect of this LHS on the

flammability, thermal stability and degradation kinetics of PMMA was investigated via cone calorimetry and thermogravimetric analysis. The addition of 3–10% by mass of ZHTMDBB to PMMA resulted in significant reduction of peak heat release rate (22–48%) of the polymer and improvements in thermal stability were observed in both air and nitrogen. Effective activation energies for the degradation process were evaluated using Flynn-Wall-Ozawa, Friedman, and Kissinger methods. All three methods indicated that the additive increased the activation energies of the first step of the degradation process in both air and nitrogen. Activation energies of the second step were lowered in nitrogen but were not significantly affected in air.

Keywords: Layered hydroxy salt, Nanocomposites, PMMA, Thermal stability, Degradation kinetics.

1. Introduction

Synthetic polymeric materials (SPMs) have found widespread industrial and domestic use because of their favorable properties which include low weight, high strength, and ease of processing; these properties have seen SPMs replacing traditional materials such as wood, and metals [1]. The major disadvantage of SPMs is that they are flammable; decreasing their flammability has become a major area of research. Flammability and thermal stability of polymers can be improved by blending virgin polymers with flame retardant (FR) additives. Halogen based FR were found to be effective in reducing the flammability of polymer [2] and [3], but they have negative impacts on the environment [4] and [5].

Major advances have been made in the search for halogen-free FR with the use of nanomaterials such as metal oxides, metal hydroxides, and metal salts being reported in the literature [6], [7] and [8]. Cationic clays which include montmorillonite (MMT) have been the most widely studied nanomaterials and have been shown to greatly improve selected fire properties of polymeric materials [9] and [10]. Recently another class of layered materials, anionic clays, have also generated interest as potential fire retardants and the most widely investigated materials in this class are the layered double hydroxide (LDH) [11] and [12]. LDHs are materials which are related to the mineral hydroxalite and have a general formula which is represented as $[M^{2+}_{1-x}M^{3+}_x(OH)_2]A^{n-}_{x/n} \cdot yH_2O$, where M^{2+} is a divalent

cation such as Ca^{2+} , Cu^{2+} , Mg^{2+} , Co^{2+} or Zn^{2+} and M^{3+} is a trivalent cation such as Fe^{3+} , Al^{3+} or Cr^{3+} with A^{n-} being an exchangeable charge compensating anion of charge n which controls the interlayer space. The anion can be inorganic such as NO_3^- , CO_3^{2-} , Cl^- or organic such as carboxylates (RCOO^-). Efforts to exploit the tunability of these structures for FR applications include varying the identity/chemical nature of the anion in the gallery as well as changing the intralayer metal ions composition [13], [14], [15] and [16].

Other closely related classes of anionic clays, hydroxy double salts (HDS) and layered hydroxy salts (LHS), although not extensively studied as LDH, have similarly been shown to have potential as fire retardants [17], [18] and [19]. In HDSs and LHSs, the metal hydroxide layers are composed of divalent cations represented as M^{2+} and Me^{2+} and are formulated as $[\text{M}^{2+}_{1-x} \text{Me}^{2+}_{1+x} (\text{OH})_{3(1-y)}]^{x+} (\text{A}^{n-}_{(1+3y)n}) \cdot m \text{H}_2\text{O}$. As in LDHs, A^{n-} is an exchangeable anion of charge n which can be inorganic or organic. HDSs and LHSs differ in that whereas in HDSs, M^{2+} and Me^{2+} are different divalent cations, in LHSs there is only a single divalent metal cation ($\text{M}^{2+} = \text{Me}^{2+}$). The LDH, HDS and LHS layers have a brucite $\{\text{Mg}(\text{OH})_2\}$ type structure in which magnesium ions are surrounded by six hydroxide ions in an approximately octahedral geometry [20]. As is the case with LDHs, these materials offer the possibility of varying the identity of both the metal constituents and the exchangeable interlayer anion in order to enable tuning physic-chemical properties of the materials in order to optimize their performance for selected applications. Work in this lab has shown that copper-based LHSs resulted in lowering of total heat release (THR) [19] as compared to LDHs which mostly resulted in lowering of peak heat release rate (PHRR) [13]. The fact that significant reduction in THR of up to 30% can be achieved using LHS [19] suggests that with careful choice of metal ion(s) and interlayer anions, a system can be obtained in which reductions in both THR and PHRR may be achieved. However, more work is necessary with single-metal-containing materials to better understand the role of metal ions in thermal/fire degradation processes.

Boron and boron-containing compounds such as zinc borate have been extensively investigated and enhanced fire performances, when combined with other additives, have been reported [21]. In this study, a zinc-based LHS with a boron-containing exchangeable anion

was prepared and compounded with PMMA using melt intercalation to produce PMMA composite. The fire properties of the PMMA composites were evaluated using cone calorimetry. Thermogravimetric analysis (TGA) derived degradation kinetics of the PMMA composites and a correlation between observed activation energies and thermal stability was also investigated.

2. Experimental

2.1. Materials

Poly (methyl methacrylate) (PMMA) {MW 120,000, T_g 99.0 °C, viscosity 0.200} containing <5.0% toluene, sodium hydroxide (flakes, 98%) and zinc nitrate hexahydrate, 99% [Zn(NO₃)₂ 6H₂O] were all obtained from Sigma Aldrich Chemical Co; Zinc oxide (99%), was obtained from Mallinckrodt Baker inc; 4-(4,4,5,5-Tetramethyl-1,3,2-dioxaborolan-2-yl) benzoic acid, 97% [C₁₃H₁₇BO₄] was purchased from Strem chemicals, Inc. All chemicals were used without further purification.

2.2. Synthesis of filler material

The precursor layered material, zinc hydroxy nitrate (ZHN), was prepared according to established methods [22]. In a typical experiment, zinc oxide (8.1 g, 0.1 mol) was added to 100 cm³ of a 2.4 M aqueous zinc (II) nitrate solution with vigorous stirring at room temperature for 24 h. The resultant white precipitate was filtered, washed several times with deionized water and dried in a vacuum oven for 48 h at about 50 °C. {4-(4,4,5,5-tetramethyl-1,3,2-dioxaborolan-2-yl) benzoate (TMDBB)}, the exchange anion to be exchanged for the NO₃⁻ anion in ZHN, was prepared by reacting the acid {4-(4,4,5,5-tetramethyl-1,3,2-dioxaborolan-2-yl) benzoic acid, (TMDBBH)} with an equimolar amount of sodium hydroxide in a volume of deionized water to make a 0.15 M solution. Converting TMDBBH to TMDBB is a necessary step to improve its solubility in water. The exchange reaction was accomplished by reacting ZHN (0.1 g) with 3.75 cm³ of a 0.15 M solution of TMDBB at 40 °C for 48 h with frequent stirring. The exchange product was filtered, washed several times with deionized water and dried at 50 °C in a vacuum oven for 48 h. The exchange product is referred herein as ZHTMDBB.

2.3. Nanocomposite preparation

The composites of PMMA and ZHTMDBB were prepared via melt blending. In this procedure, PMMA and the corresponding amount of ZHTMDBB (to give the desired percent loading) were thoroughly mixed and placed in a Brabender Plasticorder chamber at a temperature of 185 °C. The screw speed was set to 60 rpm and the blending time was 10 min. The molten composites were removed after melt blending and allowed to cool to room temperature. A reference sample of pure PMMA was subjected to the same treatment in the Brabender; without any additive. The resultant composites are identified as PMMA/ZHTMDBB-*n*, with *n* indicating the percent additive loading by mass. For example, 90 g of PMMA was mixed with 10 g ZHTMDBB to give an additive loading of 10% resulting in a composite referred to as PMMA/ZHTMDBB-10. Additive loadings were 3%, 5%, and 10% giving composites referred herein as PMMA/ZHTMDBB-3, PMMA/ZHTMDBB-5 and PMMA/ZHTMDBB-10.

2.4. FTIR and elemental analysis

Fourier transform infrared (FTIR) spectroscopy of the layered materials and the composites were obtained on a Perkin Elmer Spectrum 100 FTIR spectrometer operated at a 2 cm⁻¹ resolution in the 4000–650 cm⁻¹ spectral range; 16 scans were averaged. The FTIR spectra were recorded using a single reflection ATR accessory with a ZnSe prism (PIKE MIRacle™, from PIKE technology). Elemental analysis was carried out by Huffman labs, Colorado, using atomic emission spectroscopy interfaced with inductively coupled plasma (AES-ICP) for metal determination.

2.5. Powder X-ray diffraction

Powder X-ray diffraction (PXRD) measurements were recorded on a Rigaku Miniflex II diffractometer using Cu K α ($\lambda = 1.54 \text{ \AA}$) radiation source at 30 kV and 15 mA. The patterns were recorded in the 2θ range of 2.0° – 45.0° for powders and 2.0° – 10° for composites, data acquisition was performed using a step size of 0.083° per second. Powder samples were pressed in to the trough of the glass sample holders while polymer samples were compression molded into thin rectangular plaques and mounted on aluminum sample holders.

The diffractometer was calibrated using a silicon reference material (RSRP-43275G: manufactured by Rigaku Corporation).

2.6. Thermogravimetric analysis

Thermogravimetric analysis (TGA) and differential thermal analysis (DTA) were performed on an SDT 2960 Simultaneous DTA–TGA instrument. Samples in the range of 11.0 ± 0.2 mg were cut into small pieces of approximately 100×120 mm and 0.4 mm thickness and heated in an aluminum crucible. Data were acquired from 50 °C to 800 °C under a constant flow of nitrogen or air, at a heating rate of 20 °C/min. For polymer kinetic analysis, various heating rates ranging from 5 °C/min to 25 °C/min were used. To study the effect of sample weight on kinetic parameters, samples containing 10% loading of the additive were used. Samples with total masses in the range of 5–20 mg were heated under nitrogen atmosphere. Measurements were performed in triplicates and the average was reported here, the temperature for a given mass loss is generally reproducible to ± 3 °C [10].

2.7. Flammability test

Flammability analysis of the pure polymer and its composites were conducted on an Atlas Cone 2 instrument at an incident heat flux of 50 kW/m² with the samples in a horizontal orientation analysis. The samples were compression molded into square plaques of uniform size (100 mm \times 100 mm \times 3 mm) and weighing about 30 g. The reported values for each sample were the average of three measurements. The results from the cone calorimeter are generally considered to be reproducible to $\pm 10\%$ [23]. Bright image field transmission electron microscopy (TEM) images were collected at 60 kV using a Zeiss 10c electron microscope.

3. Results and discussion

3.1. Characterization of filler material

The structure of the interlayer anion in ZHTMDBB, 4-(4,4,5,5-Tetramethyl-1,3,2-dioxaborolan-2-yl) benzoate (TMDBB), is shown in Fig. 1. The elemental compositions of ZHN and ZHTMDBB, as obtained

from elemental analyses, are as follows: ZHN, 54.11% Zn, 3.52% N, 1.88% H, < 0.05% C corresponding to the formula $Zn_{6.5}(OH)_{11.2}(NO_3)_2 \cdot 1.8H_2O$; and ZHTMDBB, 43.84% Zn, 2.73% H, 17.28% C, 1.98% B, < 0.02% N consistent with the formula $Zn_{3.6}(OH)_{6.7}(C_{13}H_{16}BO_4)_{0.6}1.7H_2O \cdot 0.4BO_2$ indicating that there may have been some decomposition of TMDBB during the anion exchange process. The elemental composition for ZHTMDBB indicates that the nitrogen level was insignificant suggesting complete exchange.

Infrared spectra of ZHN and ZHTMDBB are shown in Fig. 2, trace (a) and trace (b) respectively. For both ZHN and ZHTMDBB, the OH stretch of the hydroxy group appears in the region from 3300 cm^{-1} to 3700 cm^{-1} . For ZHN, the sharp band at approximately 3576 cm^{-1} can be assigned to stretching vibrations of free layer hydroxy groups and the band at about 3472 cm^{-1} is due to the stretching of layer hydroxyl groups that are hydrogen bonded to the interlayer nitrate anion or water molecules. The broad band at about 3300 cm^{-1} can be assigned to the stretching of water hydroxyl groups, suggesting that ZHN has interlayer water molecules [22]. These assignments can also be used to describe the OH vibrations in ZHTMDBB. Fig. 2 trace b shows that after the exchange reaction, the characteristic asymmetric stretch of free nitrate ion at about 1372 cm^{-1} in ZHN had disappeared and a new set of peaks at 1398 cm^{-1} $\nu(B-O)$, 1580 cm^{-1} $\nu_{\text{asym}}(C=O)$ and 1533 cm^{-1} $\nu_{\text{sym}}(C=O)$ [22] and [24] appeared indicating that the nitrate group was completely exchanged with the TMDBB anion, this is in agreement with results of elemental analysis.

Fig. 3 shows an overlay of the PXRD patterns for ZHN and ZHTMDBB after anion exchange. Both materials show intense $00l$ ($l = 1-3$) reflections which are equally spaced indicating that the materials are layered and possess high range ordering, at least to the third order in the c direction. The XRD profile of ZHN indicates an interlayer distance of $0.97 \pm 0.01\text{ nm}$ and matches literature values [22]. From the Bragg equation, the new peaks ($001-003$) appearing upon exchange of nitrate with TMDBB correspond to an average d -spacing of $1.452 \pm 0.003\text{ nm}$. The absence of the nitrate reflections from the ZHTMDBB trace indicates that the exchange was complete, confirming results from elemental analysis and FTIR analysis. The increase of the interlayer space, from $0.97 \pm 0.01\text{ nm}$ in ZHN to $1.452 \pm 0.003\text{ nm}$ in ZHTMDBB is consistent with a smaller NO_3^- anion

(thermochemical radius = 1.65Å) being replaced by a larger TMDBB anion (chain length = 10.9Å). The chain length of TMDBB ion was calculated utilizing the Gaussian 98 program [25] and carried out at the DFT (B3LYP) level of theory with 6-31 + G* basis set. The chain length was calculated as the inter-atomic distance between the carboxyl oxygen and the hydrogen atom of the furthest methyl group. Estimation of crystallite sizes was performed using the Scherrer equation:

$$\tau = \frac{\kappa\lambda}{\beta\cos\theta} \quad (1)$$

where τ is the crystallite size, κ is a constant (shape factor = 0.9 for powders), β is the full width at half maximum of the diffraction peak after correcting for instrumental broadening. λ is the X-ray wavelength. The silicon 111 peak at 28.4° was used to correct for instrumental broadening. The 001 sample peaks were used to estimate the crystallite size in the c-axis dimension: 60 ± 3 nm for ZHN and 42 ± 1 nm for ZHTMDBB.

Fig. 4 shows the thermal analysis plot for ZHTMDBB, obtained at a heating rate of 20 °C/minute. The DTG indicates that there is weight loss from 50 to 150 °C, corresponding to the loss of intercalated water. The weight loss at about 210 °C, corresponding to about 10% weight loss, can be assigned to the loss of adsorbed anion or the acid form of TMDBB. The decomposition of TMDBB and dehydroxylation occur simultaneously at 430 °C. The TG shows that the decomposition of ZHTMDBB results in 65% inorganic residue at the end of the thermal decomposition process. The inorganic content obtained from TG is in agreement with the value of 68% calculated from elemental analysis results, assuming that the degradation process results in the formation of zinc oxide (ZnO) and zinc borate (ZnB₂O₆).

3.2. Characterization of filler-polymer nanocomposite

Fig. 5 shows PXRD profiles of ZHTMDBB and polymer composites. When ZHTMDBB was compounded with PMMA during melt blending, new reflections were observed at lower 2 theta values for all the three loadings with the interlayer distance (d-spacing) increased from 1.452 ± 0.003 nm for ZHTMDBB to 1.88 ± 0.05 nm for the composites. This is consistent with some degree of intercalation of the polymer into the LHS gallery. The PXRD patterns in Fig. 5 show at

least two orders of reflections indicating that the layered structure of the LHS was maintained during the compounding process. XRD alone is insufficient to characterize the quality of dispersion of the additive in a polymer matrix; transmission electron microscopy (TEM) is required since it provides direct imaging of the composites allowing visualization of the additive dispersion. Fig. 6 shows the TEM images for all the composites at both low and high magnifications. The low magnification provides information about the dispersion of the layered material in the polymer matrix while higher magnification shows whether there was intercalation or exfoliation. The TEM images at low magnification in Fig. 6 are consistent with poor dispersion and formation of microcomposites, thus good nanodispersion was not achieved here. At higher magnification, the metal hydroxide sheets, which are represented by the dark regions, seem to have aggregated and formed tactoids, which increased with increase in the additive loading.

3.3. Thermogravimetric analysis

The method of producing composites via the melt blending method has been shown not to result in significant degradation of commercial PMMA (MW 120,000) [13]. Results from thermogravimetric analysis of PMMA and its composites degraded in air and nitrogen at a heating rate of 20 °C per minute are shown in Fig. 7 and Fig. 8 respectively. The plots show that pure PMMA (commercial; MW 120,000) degradation under the heating profiles used here is a two step process regardless of the atmosphere being used which is in agreement with results obtained by other workers [26]. The two steps in the degradation of PMMA have been attributed to scission at the vinyl terminated end and to random scission of the PMMA back bone respectively [27]. The initial stabilization of PMMA in air, although not very distinct in this work, has been reported elsewhere [28] and [29]. Hirata and core workers [28] have attributed the stabilization of PMMA at early stage to the modification of the terminal double bond in PMMA, by oxygen, which results in the suppression of the end initiation process. The destabilization of PMMA by oxygen at higher temperatures, the step which is due to random scission of the chain, is due to oxygen reacting with polymer chains enhancing the random scission process.

The additive has a pronounced effect on the thermal behavior of PMMA degradation in air as shown in Fig. 7a. The degradation profile changed significantly, as can be observed from the DTG curves (Fig. 7b) in which the rate of mass loss of the first step is significantly lowered in all the composites and there is a third step observed in the temperature range of 475–550 °C. The degradation in air showed that the composites were more thermally stable than the virgin polymer with the onset of degradation, corresponding to 10% conversion ($T_{0.1}$) increasing by between 32 and 44 °C, depending on additive loading, and the temperature at 50% mass loss ($T_{0.5}$) increases by between 26 °C and 31 °C. For the degradation in N_2 , shown in Fig. 8, $T_{0.1}$ was increased for all the composites by up to 9 °C and $T_{0.5}$ was increased by up to 15 °C as compared to the virgin polymer. The results obtained here indicate that the additive is more effective in air than in a nitrogen environment, these results are in agreement with those reported by Lee and Viswanath, who used aluminum nitride and alumina as additives [30], and Laachachi and coworkers, who used ZnO, Cloisite 30B [7] and antimony oxide [31] as additives. Wang et al. have attributed the increased stability of PMMA in air, as compared to nitrogen, to the stabilization of free radicals by the inorganic compounds [32]. Increased thermal stability of PMMA when compounded with anionic clays has been reported elsewhere [13], [14] and [33].

Details of the thermal properties of PMMA and its composites are summarized in Table 1 and Table 2. The expected char yield was calculated from the amount of char remaining from the separately measured degradation of ZHTMDBB and pure PMMA. The percent loading of the additive was then factored in to calculate the individual contribution of the polymer and the additive. The results show that, under pyrolysis conditions, the amount of char remaining is significantly higher than the expected char yield suggesting that under these conditions, the additive enhances char formation. The char yields for the degradation in air are lower than those obtained in nitrogen and almost equal to the expected yield indicating that under thermo-oxidative conditions there is complete degradation of PMMA, these results are in agreement with those obtained by other workers [32], [34] and [35]. Degradation of PMMA mainly results in the formation of the monomer (MMA) which is transported from the bulky material to the surface as bubbles rather than by diffusion [36].

Although the transport of monomer does not limit the weight loss for pure PMMA, the formation of char or inorganic residue in the composites provides a barrier to the transport of MMA and should result in the transport process limiting the mass loss. The mixing of the polymer with the additive, which has about 65% inorganic content by mass, may result in the increase of thermal capacity which, together with the barrier to heat transfer due to char formation, leads to degradation of the composites occurring at higher temperatures than the pristine PMMA.

Fig. 9 shows mass difference curves, Δ mass % (difference between mass % of composites and pure PMMA) for composites in both air and nitrogen. A positive profile of the mass difference curve indicates that the composites are more stable than the pure polymer at a given temperature and the additive has thus enhanced the thermal stability of the polymer. Conversely negative profiles indicate a destabilization effect of the additive. At all levels of loadings, in both air and nitrogen, the profiles are positive in the entire temperature regime indicating that the additive has a stabilizing effect for the entire degradation temperature range. The graphs also clearly show the effect of the additive in different environment, as the environment is changed from air to nitrogen the maximum stabilization temperature shifts from around 300 °C to 420 °C and the stabilization effect is lower in nitrogen as compared to air.

3.4. Kinetic analysis

In order to get a better understanding of the degradation process and the effect of the additive on the thermal stability of PMMA, it is useful to determine kinetic parameters for the degradation process. The parameter generally found to be most useful in explaining the degradation process is the effective activation energy (E_a) which can be evaluated by carrying out kinetic analysis of the solid state reaction. For thermal methods of analysis, the techniques mainly used for the kinetic analysis are thermogravimetry (TG), differential scanning calorimetry (DSC) and differential thermal analysis (DTA). Both isothermal and non-isothermal methods can be used in kinetic experiments. Isothermal methods have a disadvantage because the sample requires time to reach the prescribed temperature and, during the temperature ramping process, the sample might undergo

transformations that are likely to affect the results, therefore the process is restricted to lower temperatures.

The methods usually employed in solid state kinetic analysis can be grouped into two; namely model fitting and isoconversional (model-free) methods. Model-fitting methods have the inherent disadvantage of producing average (global) activation energies for the entire degradation process. Isoconversional methods do not suffer from that drawback and enables the determination of the dependency of E_a on the extent of reaction and are therefore favored over model-fitting methods [37], [38] and [39]. Both isothermal and non-isothermal methods have been used in the determination of kinetic parameters in the degradation of polymers [17], [29], [40], [41] and [42].

Dynamic thermogravimetric analysis was employed in this study to calculate the E_a of PMMA and its composites by making use of the multiple heating rate kinetics (MHRK). Accordingly, a series of experiments were conducted at varying heating rates ranging from 5 °C/min to 25 °C/min. The Flynn-Wall-Ozawa method [43] incorporating Flynn's correction to the Doyle approximation [44] (referred herein as the cFWO method) together with the Friedman [45] and the Kissinger [46] methods were used in the calculation of the E_a .

The Flynn-Wall-Ozawa method can be written in a simplified form expressed as:

$$\log f(\alpha) = \log\left(A\frac{E_a}{R}\right) - \log(\beta) - 2.315 - 0.4567\left(\frac{E_a}{RT}\right) \quad (2)$$

In the above expression, $f(\alpha)$ is a conversional functional relationship; A is the pre-exponential factor (min^{-1}); E_a is the activation energy (kJ mol^{-1}); R is the molar gas constant; β is the heating rate ($^{\circ}\text{C/min}$) and T is the temperature (K).

The above equation can be rewritten as follows [41];

$$\log(\beta) = -0.4567\left(\frac{E_a}{RT}\right) + \text{constant} \quad (3)$$

From the linear form above, the isoconversional plot of $\log(\beta)$ vs $1/T$ should result in a straight line in which the E_a can be extracted from the slope. To obtain this simple equation, Flynn, Wall and Ozawa utilized the Doyle's approximation of the exponential integral [47], however this may result in significant errors of the calculated activation energies. Flynn proposed a correction to the Doyle's approximation by using tabulated correction factors, which reduces the error of the calculated E_a [44]. Fig. 10 shows a plot of the E_a , estimated from the isoconversional plots for the degradation of PMMA and the composites in nitrogen. The TGA and DTG curves for the degradation of PMMA and the composites in nitrogen (Fig. 8) shows that the degradation occurs in two steps which were assigned to end initiation from the unsaturated double bonds at the end of the chain and random scission of the chain respectively [27]. The onset of the degradation process for pure PMMA, which corresponds to 10% mass loss, has an E_a value of 143 kJ mol⁻¹. The E_a value increases gradually as the degradation process continues up to a value of 168 kJ mol⁻¹ at 30% conversion, and then drops to 164 kJ mol⁻¹ at 35% conversion, which corresponds to the transition from the first step to the second step of degradation. The E_a then increases to 184 kJ mol⁻¹ at 40% conversion as the second step of degradation start, and this increase is maintained throughout the latter part of the process up to a value of 329 kJ mol⁻¹ at 90% conversion. The results obtained here are consistent with the mechanism of PMMA degradation whereby the first step is initiated from weak links therefore has a lower E_a than the second step which is due to random C-C scission.

Hu and Chen [48] carried out a study to determine the effect of weak links on the degradation of PMMA polymerized by using different initiators {lactams, thiols and 2,2'-azobisisobutyronitrile (AIBN)} producing PMMA with different end groups. Free radically polymerized PMMA had unsaturated end group and degraded in two steps; they observed that the activation energy of the first step was lower than that of the second step (151–146 kJ mol⁻¹ for 5–20% weight loss as compared to 218–222 kJ mol⁻¹ for 80–90% weight loss). The E_a values obtained by Hu and Chen [48] agree qualitatively with those obtained in this work in that the first step has lower activation energy than the second step. The same general trend was also observed by Peterson et al. who reported effective E_a values of 190 kJ mol⁻¹ for the first step and 230 kJ mol⁻¹ for the second step [29]. Hirata et al. [28] did

isothermal analysis of PMMA (obtained by free radical polymerization) and concluded that both steps follow first order kinetics with activation energy of the first step lower than that of the second step (31 kJ mol⁻¹ and 210 kJ mol⁻¹ respectively). The low E_a for the first step has, however, been attributed to volatilization of impurities by Holland and Hay [49]. It is important to note that the activation energies of the degradation process depend largely on the polymerization methods which determine the nature of end groups [49].

The effect of the additive can clearly be seen in Fig. 10, in which the composites have a significantly higher initial E_a at low conversion, corresponding to the first step of degradation, and lower activation energy towards the end of the reaction. The E_a of the composites at 3% and 10% loading show the same trend and the E_a values are not significantly different, this suggests that the level of additive loading does not have a significant effect on the E_a values. The activation energy of the composites are higher at the onset of degradation (10% conversion) with PMMA/ZHTMDBB-10 having a value of 190 ± 10 kJ mol⁻¹ and that of pure PMMA being 142 ± 4 kJ mol⁻¹. During the early part of the second degradation step, the E_a values of the composites and pure PMMA are not significantly different up to 80% conversion where the activation energies of the composites drop below those of pure PMMA. This trend was also observed by other workers [50], and can be explained by considering that the additives act as barrier to heat and mass transfer thereby retarding the degradation process. The barrier effect require close contact between the polymer matrix and the additive, as the degradation process proceeds this close contact decreases leading to decrease of E_a of the composites. The effect of additives on the E_a of PMMA under nitrogen atmosphere has been investigated by many workers and the general trend of additives increasing the E_a has been observed, some additives increasing the E_a over the entire degradation process [35], [50], [51] and [52].

The dependence of E_a on the extent of reaction for the degradation of PMMA and its composites in air is shown in Fig. 11 which indicates that the degradation in air follows the general trend as in nitrogen with the additive increasing the E_a of the first step. The activation energies of the first degradation step of the pure polymer in air are comparable to those in nitrogen, ranging from 136 to

148 kJ mol⁻¹ in air and 136–164 kJ mol⁻¹ in nitrogen for 5–35% conversion. The activation energies of PMMA in air at higher conversions, corresponding to the second degradation step, are significantly lower than those obtained in nitrogen. These results are consistent with those obtained by Chang and Wu [34] who observed that the E_a in air at low conversion was significantly higher than in nitrogen (217–172 kJ mol⁻¹ in air and 125–160 kJ mol⁻¹ in N₂ for conversions of 10–30%). The order reversed at higher conversions (145–140 kJ mol⁻¹ in air and 175–190 kJ mol⁻¹ in N₂ for 40–70% conversion), with the transition being at about 35% conversion. This is consistent with the effect of oxygen on the degradation of PMMA; oxygen has been postulated to have a stabilizing effect on the first step and a destabilization effect on the second step [29]. The additive had the effect of increasing the activation energy of the first step of degradation, but did not have a significant effect on the E_a of the second step. The additive may act by stabilizing or scavenging the free radicals generated during the initial stages of the thermal oxidative degradation process thereby increasing the barrier for reaction to occur. It was also noted that the additive resulted in much higher increases of the activation energy in air than in nitrogen (from 142 kJ mol⁻¹ to 250 kJ mol⁻¹ in air compared to 143 kJ mol⁻¹ to 190 kJ mol⁻¹ in nitrogen at 10% conversion) which is consistent with the additive stabilizing free radicals generated during thermal oxidative degradation.

The Friedman method is a differential isoconversional method for the calculation of E_a which is based on the rate of weight loss as a function of temperature. The method is based on the following equation

$$\ln \frac{d\alpha}{dt} = \ln \{A(1 - \alpha)^n\} - \frac{E}{RT} \quad (4)$$

Using the above equation, the activation energy is obtained from the slope of a plot of natural logarithms of the rate of weight loss at different heating rates against reciprocal absolute temperature at a given weight loss. Activation energies obtained using the Friedman method follow the same trend obtained by using the cFWO method. Fig. 12 shows the comparison of the Friedman method and cFWO method for the degradation of PMMA and PMMA/ZHTMDBB-10 in nitrogen. The same trend was observed for E_a values for the

degradation under air (data not shown here). The third method used to determine the activation is the Kissinger method in which only the temperature at maximum rate of weight loss is required for computing E_a [46]. The E_a is calculated according to the following expression

$$\ln\left(\frac{\phi}{T_m^2}\right) = \ln(nRAW_m^{n-1}/E) - \frac{E_*}{R} \frac{1}{T_m} \quad (5)$$

where ϕ is the heating rate, T_m is the temperature at the maximum rate of weight loss, R is the universal gas constant, E is the activation energy, A is the pre-exponential factor, W_m is the weight of the sample at the maximum rate of weight loss, and n is the apparent order of the reaction with respect to the sample weight. The E_a is obtained from the slope of a plot of $\ln(\phi/T_m^2)$ against $1/T_m$ at various heating rates. As can be seen from Fig. 7, the DTG for the first step of composites degraded in air exhibit a shoulder and it is difficult to accurately determine the exact temperature of maximum rate of degradation, as such it was not possible to calculate the activation energy for composites degraded in air. Table 3 gives a summary of the of E_a values obtained from the Kissinger method, the results are consistent with results from the cFWO and Friedman methods in that the activation for the first step in the degradation of PMMA in nitrogen is lower than that of the second step (180 kJ mol^{-1} as compared to 274 kJ mol^{-1} for the second step). Also the activation energies of the composites are higher for the first step of degradation as compared to pure PMMA, the value obtained here for the second step agrees with that obtained by Hirata et al. [28] who obtained 224 kJ mol^{-1} . The results from the Kissinger method also shows that PMMA degraded in air does not show much difference in the activation energies of the two steps which is consistent with what was obtained with the other methods.

It has also been noted that values of activation energies obtained for polymer degradation vary widely depending on molecular weight, sample thickness, polymerization conditions and sample weight used in the TGA analysis [49], [53] and [54]. For the work reported here, sample size and morphology are expected to be most important. The influence of sample weight on the degradation of PMMA/ZHTMDBB-10 in nitrogen atmosphere was investigated using sample weights (w) ranging from 5 mg to 20 mg; the data were analyzed using cFWO method. Results shown in Fig. 13 indicate that

the activation energy is not significantly different at low w (5 mg and 11 mg), but the difference is significant when w is increased to 20 mg. The results suggests that for low sample weights (5–11 mg) the mechanism of degradation remains the same or diffusion of molecules (especially products of decomposition) is not affected and product (monomer) recombination is not significant. When w was increased to 20 mg the E_a values obtained increased significantly, the increase being more pronounced during the second step of the degradation process which is due to random scission of the chain. This increase could be due to the large sample size affecting heat and/or mass transfer. Comparable results were obtained by Carrasco and Pagès who analyzed the degradation of polystyrene using TGA sample weights ranging from 6.0 to 25 mg, they observed an increase of E_a from 128 kJ mol⁻¹ to 161 kJ mol⁻¹ when the sample weight was increased from 6 mg to 25 mg [53]. Further work needs to be done to fully understand the effect of sample weight on kinetic parameters of PMMA degradation. In addition the effects of sample preparation on morphology, and subsequent impact on observed E_a , also require further investigation.

3.5. Flammability properties

The effect of the additive on the flammability of PMMA was investigated by making use of cone calorimeter. The parameters obtained from the cone calorimeter which are relevant to the evaluation of additive as flame retardant include the heat release rate (HRR), peak of HRR (PHRR), total heat release (THR), smoke production (reported here as average specific extinction area, ASEA), and time to ignition, (t_{ig}). The ideal additive will result in the lowering of PHRR, THR, ASEA, and an increase in the time to ignition (t_{ig}).

Fig. 14 shows the variation of the heat release rate as a function of the combustion time for pure PMMA, PMMA/ZHTMDBB-3, PMMA/ZHTMDBB-5, and PMMA/ZHTMDBB-10 at a heat flux of 50 kW/m². The heat flux of 50 kW/m² was chosen in an aim to simulate the radiant heat in a developing fire [55] so as to assess the fire retarding performance of the additive during the development of fire. The HRR curves for the composites are spread over a wider range as compared to pure PMMA showing that the composites burn for a longer time. The integration of the area under the respective curve for each composite and pure PMMA gives the total heat release (THR). The

additive did not significantly reduce the THR, this has been reported by other workers [14] who used LDH additives. The summary of cone calorimetry data presented in Table 4 shows that the additive resulted in a significant increase in the average smoke produced (ASEA). The amount of smoke produced increased as the level of loading increased, this could be due to the presence of benzene ring on the additive which may increase the amount of smoke produced. The important feature of Fig. 14 and the summary of results presented in Table 4 is the significant lowering of the peak heat release rate by up to 48% for PMMA/ZHTMDBB-10. The reduction of PHRR obtained here is comparable to values obtained for LDH systems [14], [26] and [33] and this shows that the LHS system studied here is equally effective in reducing PHRR of PMMA as LDH systems. The lowering of the PHRR or increase in the limiting oxygen index has been shown to correspond with the increase in the production of char for condensed phase FR [1] and [9]. Work reported by Martín et al. and Armitage et al. have shown that incorporating boron into polymers lead to an increase in char production and a corresponding increase in the limiting oxygen index [56] and [57]. The combustion process of polymers involves heating the polymer using an external heat source and this result in the decomposition of the polymer. For PMMA the initial product of the decomposition is the monomer (MMA) and small amounts of other products such as propylene and acetone [58] and [59]. The MMA molecules then further decomposes producing volatile (combustible) compounds (methane, methanol, formaldehyde and acetylene) which then undergo oxidation, releasing heat which is then fed back to the bulk polymer causing further decomposition of the polymer thereby sustaining the flame even when the external heat source has been removed. For an additive to be effective as a fire retardant, it should be able to break the above cycle. This can be achieved in a variety of ways which include; (i) improvement of thermal stability of the polymer, (ii) dilution and subsequent quenching of the flame, and (iii) providing a barrier for heat and mass transfer [41] ZHTMDBB might act by diluting and quenching the flame by generation of non combustible materials such as CO₂ and water from decomposition of the additive. In addition, the char produced during the burning process may act as a barrier to heat and mass transfer reducing the diffusion of combustible products of decomposition, or a combination of the two mechanisms.

The burning of pure PMMA is characterized by bubbling and cracking of the surface which enhances the transport of pyrolysis products to the surface thereby enhancing the degradation process [1] and [58]. The reduction in PHRR observed in this work can be attributed to char production, the char acts as a protective layer and a barrier to heat and mass transfer. With this in mind, the production of a continuous layer of char covering the whole surface should, in principle, lead to a much higher improvement in PHRR as well as other flammability measures such as the limiting oxygen index (LOI). A continuous barrier does not allow degradation products below the heated surface to be exposed to the fire during cone calorimetry test or external heat flux in the gasification process. Kashiwagi et al. [1] showed that additives which crosslinked and formed a network char structure produced better improvements in flammability behavior than additives which formed aggregates and pillars. The morphology of the char formed when anionic clays are used varies with the metal constituents of the clays, the intercalated anion and the polymer, in some instances char covering the whole surface can be obtained resulting in greater reduction in PHRR and sometimes small aggregates spread throughout the surface are observed [13] and [60].

The charring process in this work exhibited significant pillaring whereby there is initial char formation on the surface of the polymer and as the degradation continues, cracks form on the surface and bubbles from underneath the surface escape; the pillars can be observed in Fig. 15. The movement of these bubbles results in the coagulation of the char, forming discrete pillars which grew as the burning progressed. The coagulation of the char into pillars may be the results of the poor dispersion of the LHS in the polymer, as indicated by TEM images discussed previously.

The pillars obtained in this work had two distinct regions: the top part which was white/light gray in color and the lower part which was black. Samples from these two regions showed the following elemental compositions; white part: 71.81% Zn, 0.35% C, 13.65% O, 3.25% B, < 0.05% N, < 0.05% H. For the white sample at the top of the pillar, the mole ratio of Zn:B was thus found to be 3.6:1 and that of Zn:C was 37.7:1. For the black, lower part, of the pillar elemental analysis determined a relative composition of: 70.99% Zn, 0.47% C, 14.72% O, 3.01% B, < 0.05% N, < 0.05% H. In the lower part of the

pillars, the mole ratio of Zn:B was thus found to be 3.9:1 and that of Zn:C was 27.7:1. These results indicate that the black part had greater carbon content than the white part; this might be due to carbonaceous char which was formed at the lower part of the pillar. As the material started to decompose the char started to form pillars as explained above, as the char limited heat and matter transfer carbonaceous particles began to form underneath the char resulting in the black part of the char, this is supported by the idea that as the char grew carbonaceous materials were trapped under the char and the ratio of Zn:C differs in the two regions of the char. The stacking of the char can be clearly seen in Fig. 15 which shows the char formed after cone calorimetry tests, the amount of char, size of the char pillars and the surface coverage of the aluminum foil holder increased with the loading of the additive. The cracking of the char and formation of char pillars exposed the polymer and degradation products to the fire during the burning process and this resulted in the char not providing sufficient protection to effectively reduce the burning of the polymer. The char in this case served to slow the flow of combustibles thereby reducing flame intensity as shown by the reduction in PHRR, however the amount of polymeric material which is combusted is not significantly affected as evidenced by the small reduction in THR observed (Table 4).

Fig. 16 shows the XRD profile for PMMA/ZHTMDBB-10 residue/char after cone calorimetry test which reveals the presence of ZnO phase (PDF # 36-1451) and zinc borate (ZnB_2O_6) phase (PDF # 27-983) [61]. Zinc borate could have been formed by the reaction of zinc oxide and oxides of boron formed from the oxidation of boron during the burning process [62]. Since zinc borates have been shown to reduce the flammability of polymers, further studies are required to investigate the contribution of the zinc borate phase to the reduction in PHRR observed in this study.

4. Conclusions

The ZHTMDBB layered additive exhibited some intercalation by PMMA when melt blended, with poorly dispersed additive tactoids observed in TEM images. The thermal stability, degradation kinetics and fire properties of PMMA and its composites with ZHTMDBB have been studied by TGA and cone calorimetry. TGA results showed that there was significant increment in T_{10} and T_{50} for all the composites as

compared to the pristine PMMA in both air and nitrogen and the additive has more stabilizing effect in air as compared to nitrogen and this has practical benefits in that fires occurs in an oxygen environment. The degradation kinetics of PMMA and the composites showed that the additives increased the activation energies for the first step in the degradation; the activation energies of the second step in air were not significantly affected but in nitrogen the E_a was reduced at higher conversion. The activation energy for the degradation in air is lower than in nitrogen for the second step but for the first step the activation energies were not significantly different. All three methods used in this study were in agreement. The additive significantly reduced the peak heat release rate (PHRR) of PMMA, despite pillaring of the char. Similar to most LDHs, it did not reduce THR. Further optimization is necessary to decrease smoke production.

Acknowledgements

This work was performed under the sponsorship of the US Department of Commerce, National Institute of Standards and Technology, Grant 60NANB6D6018.

References

1. Kashiwagi T, Du FM, Douglas JF, Winey KI, Harris RH, Shields JR. Nanoparticle network reduce the flammability of polymer nanocomposites. *Nat Mater* 2005a;4(12):928-33.
2. Bertelli G, Camino G, Costa L, Locatelli R. Fire retardant systems based on melamine hydrobromide: part I-fire retardant behaviour. *Polym Degrad Stab* 1987;18(3):225-36.
3. Varbanov S, Peeva N, Stoeva S, Nedkov E, Borisov G. Reduction of the flammability of polypropylene by tertiary phosphine oxides containing halogenated phenoxy groups. *Eur Polym J* 1988;24(2):151-6.
4. Hajslová J, Pulkrabová J, Poustka J, Čajka T, Randák T. Brominated flame retardants and related chlorinated persistent organic pollutants in fish from river Elbe and its main tributary Vltava. *Chemosphere* 2007;69(8):1195-203.
5. Kitamura S, Kato T, Iida M, Jinno N, Suzuki T, Ohta S, et al. Anti-thyroid hormonal activity of tetrabromobisphenol A, a flame retardant. and related compounds: affinity to the mammalian thyroid hormone receptor, and effect on tadpole metamorphosis. *Life Sci* 2005;76(14):1589-601.

6. Hornsby PR, Cusack PA, Cross M, Toth A, Zelei B, Marosi G. Zinc hydroxystannate-coated metal hydroxide fire retardants: fire performance and substrate-coating interactions. *J Mat Sci* 2003;38(13):2893-9.
7. Laachachi A, Ruch D, Addiego F, Ferriol M, Cochez M, Lopez Cuesta JM. Effect of ZnO and organo-modified montmorillonite on thermal degradation of poly (methyl methacrylate) nanocomposites. *Polym Degrad Stab* 2009;94(4):670-8.
8. Morgan AB, Bundy M, Cone calorimeter analysis of UL-94 V-rated plastics. *Fire Mater* 2007;31(4):257-83.
9. Kashiwagi T, Harris RH, Zhang X, Briber RM, Cipriano BH, Raghavan SR, et al. Flame retardant mechanism of polyamide 6-clay nanocomposites. *Polymer* 2004;45(3):881 -91.
10. Zhang J, Wilkie CA. Preparation and flammability properties of polyethylene-clay nanocomposites. *Polym Degrad Stab* 2003;80(1):163-9.
11. Costa FR, Wagenknecht U, Heinrich G. LDPE/Mg-Al layered double hydroxide nanocomposite: thermal and flammability properties. *Polym Degrad Stab* 2007;92(10):1813-23.
12. Ye L, Ding P, Zhang M, Qu BJ. Synergistic effects of exfoliated LDH with some halogen-free flame retardants in LDPE/EVA/HFMH/LDH nanocomposites. *J Appl Polym Sci* 2008;107(6):3694-701.
13. Manzi-Nshuti C, Wang DY, Hossenlopp JM, Wilkie CA. Aluminum-containing layered double hydroxides: the thermal, mechanical, and fire properties of (nano)composites of poly(methyl methacrylate). *J Mater Chem* 2008;18(26):3091-102.
14. Manzi-Nshuti C, Hossenlopp JM, Wilkie CA. Fire retardancy of melamine and zinc aluminum layered double hydroxide in poly(methyl methacrylate). *Polym Degrad Stab* 2008;93(10):1855-63.
15. Nyambo C, Kandare E, Wang D, Wilkie CA. Flame-retarded polystyrene: Investigating chemical interactions between ammonium poly phosphate and MgAl layered double hydroxide. *Polym Degrad Stab* 2008;93(9): 1656-63.
16. Nyambo C, Kandare E, Wilkie CA. Thermal stability and flammability characteristics of ethylene vinyl acetate (EVA) composites blended with a phenyl phosphonate-intercalated layered double hydroxide (LDH), melamine polyphosphate and/or boric acid. *Polym Degrad Stab* 2009;94(4):513-20.

17. Kandare E, Deng HM, Wang DY, Hossenlopp JM. Thermal stability and degradation kinetics of poly(methyl methacrylate)/layered copper hydroxy methacrylate composites. *Polym Adv Technol* 2006;17(4):312-9.
18. Kandare E, Chigwada G, Wang D, Wilkie CA, Hossenlopp JM. Probing synergism, antagonism, and additive effects in poly (vinyl ester) (PVE) composites with fire retardants. *Polym Degrad Stab* 2006b;91(6):1209-18.
19. Kandare E, Chigwada G, Wang D, Wilkie CA, Hossenlopp JM. Nanostructured layered copper hydroxy dodecyl sulfate: a potential fire retardant for poly (vinyl ester) (PVE). *Polym Degrad Stab* 2006a;91(8):1781-90.
20. Miyata S. Anion-exchange properties of hydrotalcite-like compounds. *Clays Clay Miner* 1983;31(4):305-11.
21. Genovese A, Robert AS. Structural and thermal interpretation of the synergy and interactions between the fire retardants magnesium hydroxide and zinc borate. *Polym Degrad Stab* 2007;92(1):2-13.
22. Biswick T, Jones W, Pacula A, Serwicka E, Podobinski J. The role of anhydrous zinc nitrate in the thermal decomposition of the zinc hydroxy nitrates $Zn_5(OH)_8(NO_3)_2 + 2H_2O$ and $ZnOHNO_3 + H_2O$. *J Solid State Chem* 2007;180(4):1171-9.
23. Gilman JW, Kashiwagi T, Nyden M, Brown JET, Jackson CL, Lomakin S, et al. In: AI-Malaika S, Golovoy A, Wilkie CA, editors. *Flammability studies of polymer layered silicate nanocomposites: Polyolefin, epoxy and vinyl ester resins, chemistry and technology of polymer additives*. London: Blackwell Science; 1999. p. 249.
24. Addison CC, Gatehouse BM. The infrared spectra of anhydrous transition-metal nitrates. *J Chem Soc*; 1960:613-6.
25. Gaussian 98, Revision A.11.4. Frisch MJ, Trucks GW, Schlegel HB, Scuseria GE, Robb MA, Cheeseman JR, Zakrzewski VG, Montgomery JA. Jr, Stratmann RE, Burant JC, Dapprich S, Millam JM, Daniels AD, Kudin KN, Strain MC, Farkas O, Tomasi J, Barone V, Cossi M, Cammi R, Mennucci B, Pomelli C, Adamo C, Clifford S, Ochterski J, Petersson GA, Ayala PY, Cui Q, Morokuma K, Rega N, Salvador P, Dannenberg JJ, Malick DK, Rabuck AD, Raghavachari K, Foresman JB, Cioslowski J, Ortiz JV, Baboul AG, Stefanov BB, Liu G, Liashenko A, Piskorz P, Komaromi I, Gomperts R, Martin RL, Fox DJ, Keith T, AI-Laham MA, Peng CY, Nanayakkara A, Challacombe M, Gill PMW, Johnson B, Chen

W, Wong MW, Andres JL, Gonzalez C, Head-Gordon M, Replogle ES, Pople JA, Gaussian, Inc., Pittsburgh PA, 2002.

26. Manzi-Nshuti C, Songtipya P, Manias E, Jimenez-Gasco MM, Hossenlopp JM, Wilkie CA. Polymer nanocomposites using zinc aluminum and magnesium aluminum oleate layered double hydroxides: effects of LDH divalent metals on dispersion, thermal, mechanical and fire performance in various polymers. *Polymer* 2009;50:3564-74.
27. Kashiwagi T, Inaba A, Brown JE, Hatada K, Kitayama T, Masuda E. Effects of weak linkages on the thermal and oxidative degradation of poly(methyl methacrylates). *Macromolecules* 1986;19(8):2160-8.
28. Hirata T, Kashiwagi T, Brown JE. Thermal and oxidative-degradation of poly (methyl methacrylate) – weight-loss. *Macromolecules* 1985;18(7):1410-8.
29. Peterson JD, Vyazovkin S, Wight CA. Kinetic study of stabilizing effect of oxygen on thermal degradation of poly(methyl methacrylate). *J Phys Chem B* 1999;103(38):8087-92.
30. Lee YM, Viswanath DS. Degradation of poly(methyl methacrylate) (PMMA) with aluminum nitride and alumina. *Polym Eng Sci* 2000;40(11):2332-41.
31. Laachachi A, Cochez M, Ferriol M, Leroy E, Lopez Cuesta JM, Oget N. Influence of Sb₂O₃ particles as filler on the thermal stability and flammability properties of poly(methyl methacrylate) (PMMA). *Polym Degrad Stab* 2004;85(1):641-6.
32. Wang H, Xu P, Zhong W, Shen L, Du Q, Transparent poly(methyl methacrylate)/silica/zirconia nanocomposites with excellent thermal stabilities. *Polym Degrad Stab* 2005;87(2):319-27.
33. Nyambo C, Wang D, Wilkie CA. Will layered double hydroxides give nanocomposites with polar or non-polar polymers? *Polym Adv Technol* 2008;20(3):332-40.
34. Chang T, Wu KH. The effect of silicon and phosphorus on the thermo-oxidative degradation of poly(methyl methacrylate). *Polym Degrad Stab* 1997;57(3):325-30.
35. Wang HT, Meng S, Xu P, Zhong W, Du QG. Effect of traces of inorganic content on thermal stability of poly(methyl methacrylate) nanocomposites. *Key eng Mater* 2002;47(3):302-7.
36. Kashiwagi T, Du FM, Winey KI, Groth KA, Shields JR, Bellayer SP, et al. Flammability properties of polymer nanocomposites with single-walled

- carbon nanotubes: effects of nanotube dispersion and concentration. 2005b;46(2):471-81.
37. Budrugaec P, Homentcovschi D, Segal E. Critical analysis of the isoconversional methods for evaluating the activation energy. I. Theoretical background. *J Therm Anal Calorim* 2001;63(2):457-63.
 38. Popescu C, Segal E. Critical considerations on the methods for evaluating kinetic parameters from nonisothermal experiments. *Int J Chem Kinet* 1998;30(5):313-27.
 39. Vyazovkin S, Wight CA. Kinetics in solids. *Annu Rev Phys Chem* 1997;48:125-49.
 40. Gao Z, Kneko T, Dongyan H, Nakada M. Kinetics of thermal degradation of poly(methyl methacrylate) studied with the assistance of the fractional conversion at the maximum reaction rate. *Polym Degrad Stab* 2004;84(3):399-403.
 41. Chigwada G, Kandare E, Wang D, Majoni S, Mlambo D, Wilkie CA, et al. Thermal stability and degradation kinetics of polystyrene/organically-modified montmorillonite nanocomposites. 2008;8:1927-36.
 42. Lin JP, Chang CY, Wu CH, Shih SM. Thermal degradation kinetics of polybutadiene rubber. *Polym Degrad Stab* 1996;53(3):295-300.
 43. Ozawa TA. New method of analyzing thermogravimetric data. *Bull Chem Soc Jpn* 1965;38(11):1881-6.
 44. Flynn JH. The isoconversional method for determination of energy of activation at constant heating rates – corrections for the Doyle approximation. *J Therm Anal* 1983;27(1):95-102.
 45. Friedman HL, Kinetics of thermal degradation of char-forming plastics from thermogravimetry: application to a phenolic plastic. *J Polym Sci Polym Symp* 1964;6(1):183-95.
 46. Kissinger HE. Reaction kinetics in differential thermal analysis. *Anal Chem* 1957;29(11):1702-6.
 47. Doyle CD. Estimating isothermal life from thermogravimetric data. *J Polym Sci* 1962;6(12):639-42.
 48. Hu YH, Chen CY. The effect of end groups on the thermal degradation of poly (methyl methacrylate). *Polym Degrad Stab* 2003;82(1):81-8.
 49. Holland BJ, Hay JN. The effect of polymerisation conditions on the kinetics and mechanisms of thermal degradation of PMMA *Polym Degrad* 2002;77:435-9.

50. Chen K, Yang RC, Cheng SW. The kinetic analysis of thermal decomposition of PMMA/MMT nanocomposites. *Key Eng Mater* 2007;353-358:1366-9.
51. Hu YH, Chen CY, Wang CC. Viscoelastic properties and thermal degradation kinetics of silica/PMMA nanocomposites. *Polym Degrad Stab* 2004;84(3):545-53.
52. Wang GA, Wang CC, Chen CY. The disorderly exfoliated LDHs/PMMA nanocomposites synthesized by in situ bulk polymerization: the effects of LDH-U on thermal and mechanical properties. *Polym Degrad Stab* 2006;91(10):2443-50.
53. Carrasco F, Pagès P. Thermogravimetric analysis of polystyrene: influence of sample weight and heating rate on thermal and kinetic parameters. *J Appl Polym Sci* 1996;61(1):187-97.
54. Kokta BV, Valade JL, Martin WN. Dynamic thermogravimetric analysis of polystyrene: effect of molecular weight on thermal decomposition. *J Appl Polym Sci* 1973;17(1):1-19.
55. ScharTEL B, Hull TR. Development of fire-retarded materials – Interpretation of cone calorimeter data. *Fire Mater* 2007;31(5):327-54.
56. Armitage P, Ebdon JR, Hunt BJ, Jones MS, Thorpe FG. Chemical modification of polymers to improve flame retardance-I. The influence of boron-containing groups. *Polym Degrad Stab* 1996;54(2-3):387-93.
57. Martin C, Hunt BJ, Ebdon JR, Ronda JC, Cadiz V. Synthesis, polymerization, and effects on the flame retardancy of boron-containing styrenic monomers. *J Polym Sci Part A Polym Chem* 2005;43(24):6419-30.
58. Zeng WR, Li SF, Chow WK. Review on chemical reactions of burning poly (methyl methacrylate) PMMA. *J Fire Sci* 2002;20(5):401-33.
59. Zeng WR, Li SF, Chow WK. Preliminary studies on burning behavior of poly-methylmethacrylate (PMMA). *J Fire Sci* 2002a;20(4):297-317.
60. Manzi-Nshuti C, Hossenlopp JM, Wilkie CA. Comparative study on the flammability of polyethylene modified with commercial fire retardants and a zinc aluminum oleate layered double hydroxide. *Polym Degrad Stab* 2009;94 (5):782-8.
61. JCPDS, International Centre for Diffraction Data. Powder diffraction file alphabetic indexes for experimental patterns. Newton Square, PA: Inorganic Phases; 2009.

62. Hogarth CA, Ahmed MM. Infrared absorption spectroscopy of zinc borate and vanadium borate glasses. J Mater Sci Lett 1983;2(11):649-52.

About the Authors

Jeanne M. Hossenlopp : Department of Chemistry, Marquette University, P.O. Box 1881, Milwaukee, WI 53201-1881, USA

Tel.: +1 414 288 3537; fax: +1 414 288 7066.

Email: Jeanne.hossenlopp@marquette.edu

Appendix

Table 1: Summary of TGA data for pure PMMA and nanocomposites at 20 °C/min in N₂

Sample	T ₁₀ (°C)	T ₅₀ (°C)	ΔT ₅₀ (°C)	Char (%) (expected)
Pure PMMA	284 ± 1	374.1 ± 0.5	—	0.78 ± 0.05
PMMA/ZHTMDBB-3	289 ± 0.5	384 ± 1	10 ± 1	4.0 ± 0.1 (2.6)
PMMA/ZHTMDBB-5	290 ± 1	385 ± 1	11 ± 1	6.5 ± 0 (3.9)
PMMA/ZHTMDBB-10	293.0 ± 0.5	389 ± 0.5	14.9 ± 0.7	9.8 ± 0 (7.0)

Note: T₁₀, temperature at which 10% mass loss occurs and is regarded as the onset of degradation; T₅₀, temperature at which 50% mass loss occurs; ΔT₅₀ difference between T₅₀ of the composite and pure PMMA. Entries in italics are the expected char based on the residue obtained during the decomposition of ZHTMDBB and pure PMMA samples.

Table 2: Summary of TGA data of pure PMMA and nanocomposites at 20 °C/min in air

Sample	T ₁₀ (°C)	T ₅₀ (°C)	ΔT ₅₀ (°C)	Char (%) (expected)
Pure PMMA	269.9 ± 0.8	356 ± 1.5	—	0.65 ± 0.08
PMMA/ZHTMDBB-3	303 ± 2	382 ± 1	26 ± 1	2.2 ± 0.4 (2.0)
PMMA/ZHTMDBB-5	311 ± 3	383.7 ± 0.8	27 ± 1	3.6 ± 0.1 (3.6)
PMMA/ZHTMDBB-10	314.0 ± 0.8	387.1 ± 0.8	31 ± 1	7.0 ± 0.1 (6.7)

Note: T₁₀ temperature at which 10% mass loss occurs and is regarded as the onset of degradation; T₅₀, temperature at which 50% mass loss occurs; Δ T₅₀ difference between T₅₀ of the composite and pure PMMA. Entries in italics are the expected char based on the residue obtained during the decomposition of ZHTMDBB and pure PMMA samples.

Table 3: Summary of E_a values obtained from the Kissinger method

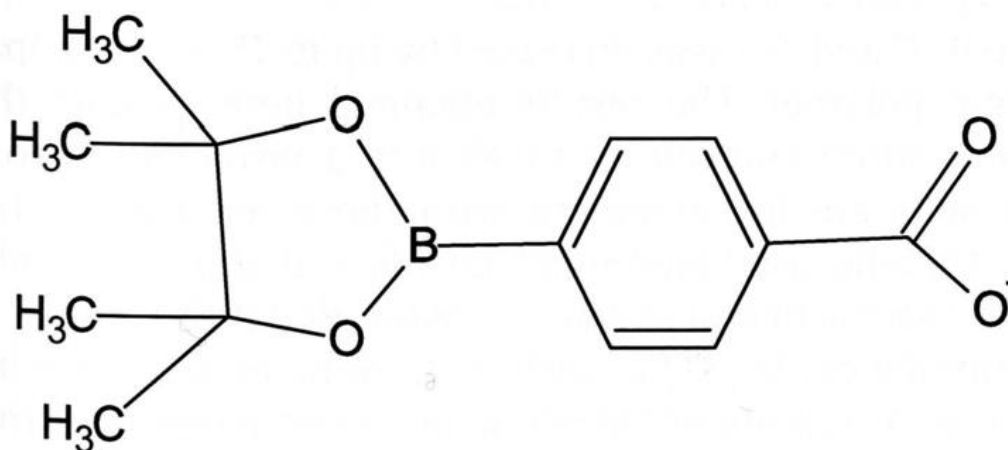
	E_a (kJ mol ⁻¹) in nitrogen		E_a (kJ mol ⁻¹) in air	
	First step	Second step	First step	Second step
Pure PMMA	180 ± 8	274 ± 6	138 ± 8	152 ± 4
PMMA/ZHTMDBB-10	225 ± 6	220 ± 13	—	—
PMMA/ZHTMDBB-3	212 ± 6	304 ± 18	—	—

Note: The composites in air did not have a distinct first degradation peak so it was not possible to calculate the activation energies.

Table 4: Summary of the cone calorimetry data

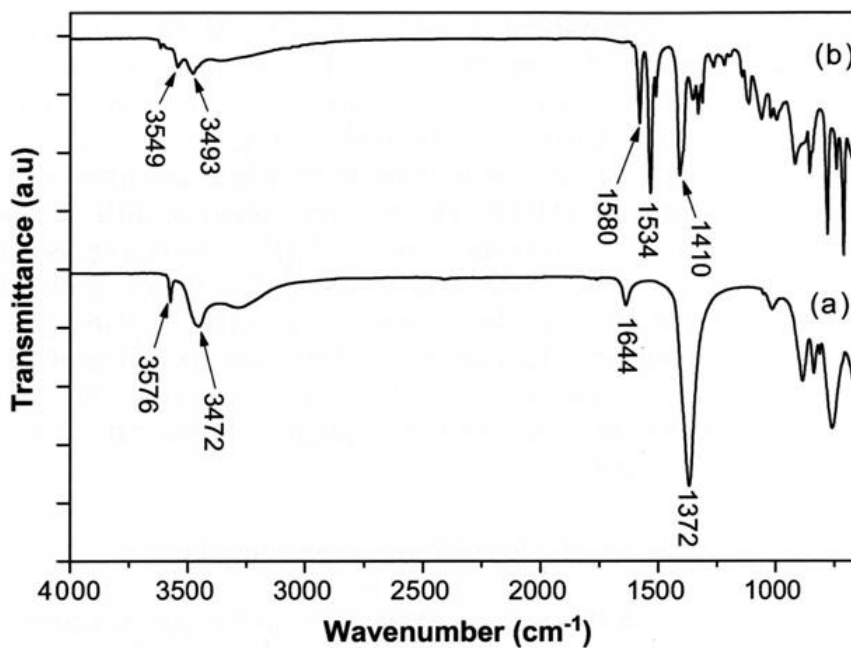
Sample	TSC (s)	PHRR (kW/m ²) (% red)	T _{PHRR} (s)	THR (MJ/m ²) (% red)	AMLR (g/secm ²)	ASEA (m ² /kg)
Pure PMMA	10 ± 2	1092 ± 29	93 ± 4	79.9 ± 0.7	31 ± 4	134 ± 8
PMMA/ZHTMDBB-3	7 ± 1	849 ± 73 (22)	90 ± 3	77.0 ± 0.7 (3.7)	33 ± 5	179 ± 12
PMMA/ZHTMDBB-5	8 ± 2	646 ± 6 (41)	91 ± 5	75.5 ± 0.4 (5.0)	24 ± 0	192 ± 2
PMMA/ZHTMDBB-10	9 ± 1	568 ± 34 (48)	96 ± 1	72.4 ± 0.2 (10.0)	19 ± 1	201 ± 27

Fig. 1.



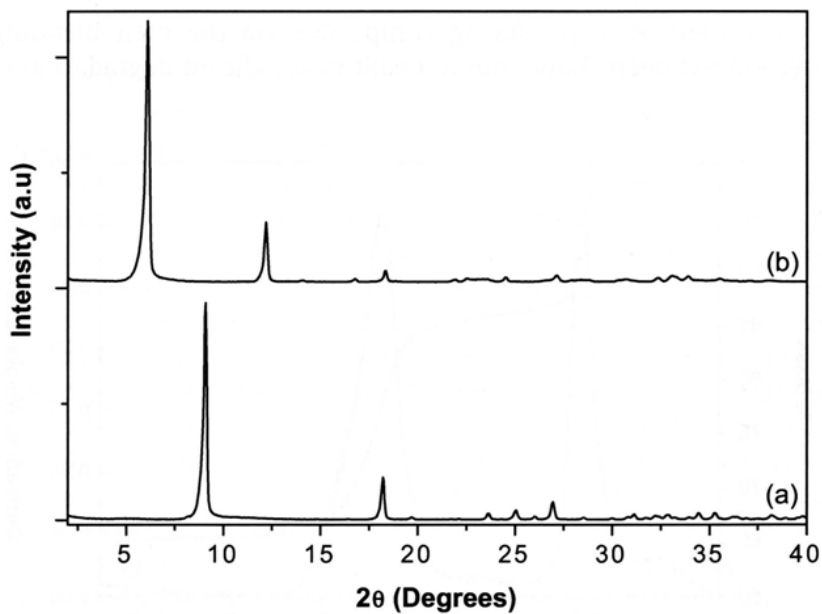
Chemical structure of 4-(4,4,5,5-Tetramethyl-1,3,2-dioxaborolan-2-yl) benzoate (TMDDBB).

Fig. 2.



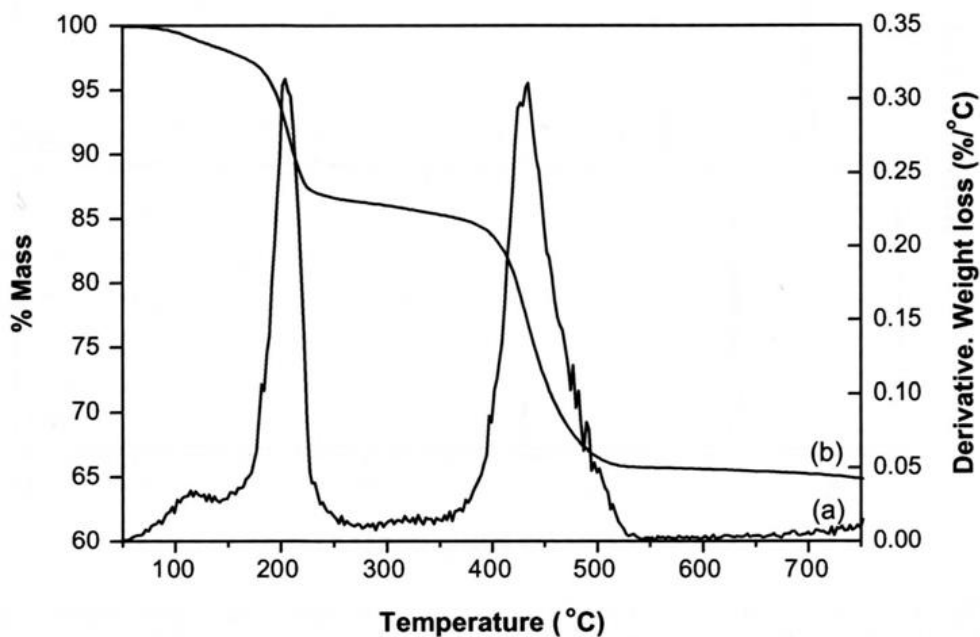
FTIR spectra of zinc hydroxy nitrate LHS (trace a) and zinc hydroxy TMDBB LHS (trace b). Traces are offset for clarity but not otherwise scaled.

Fig. 3.



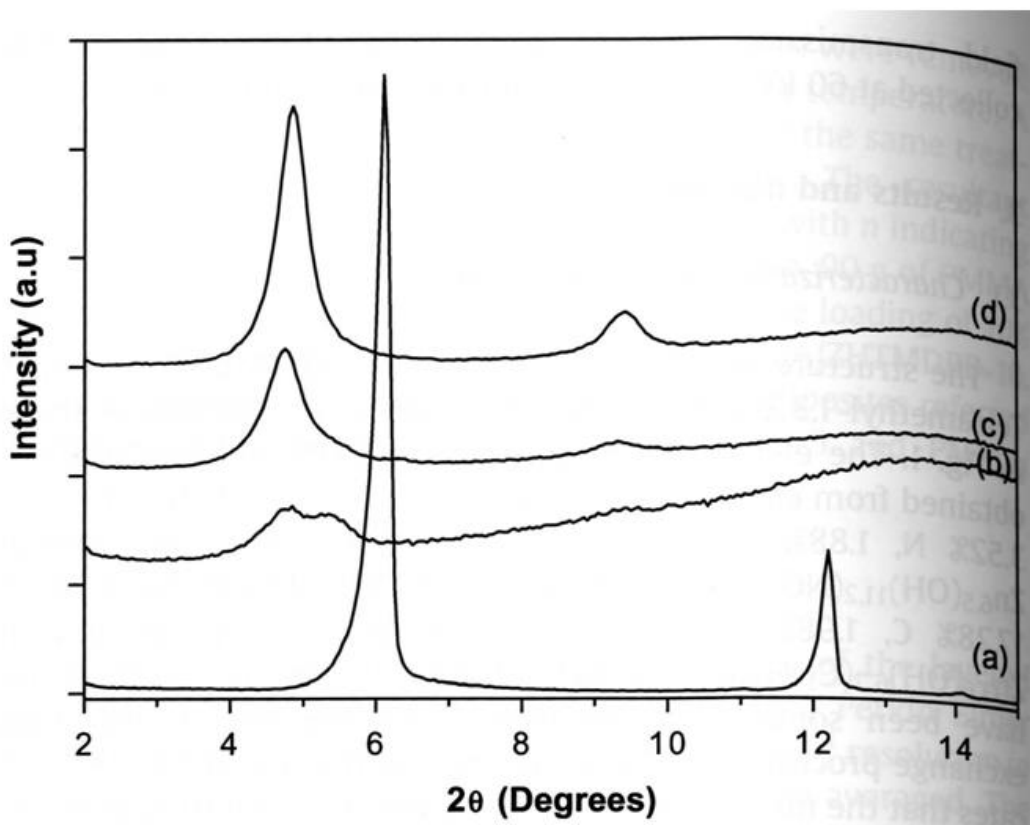
Powder x-ray diffraction data for (a): ZHN which has been indexed as $\text{Zn}_5(\text{OH})_8(\text{NO}_3)_2 \cdot 2\text{H}_2\text{O}$ and JCPDS file 24-1460 with basal spacing of 0.98 nm and (b): ZHTMDBB with a basal spacing of 1.45 nm. Traces are offset for clarity but not otherwise scaled.

Fig. 4.



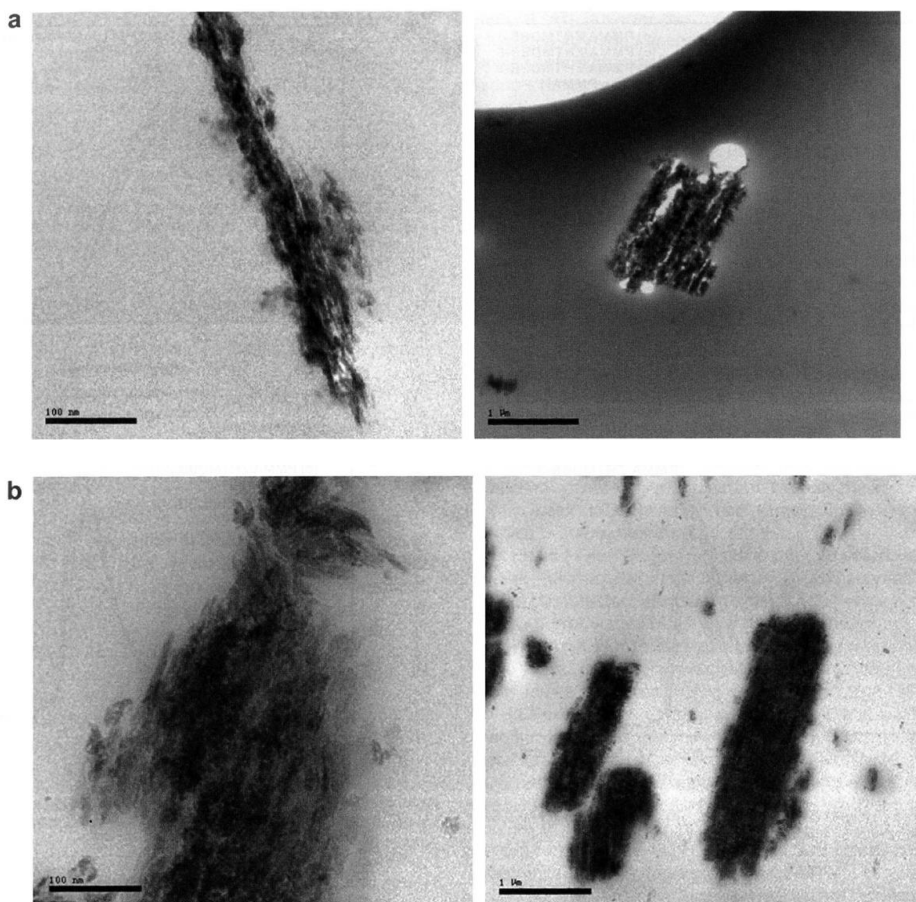
(a) DTG and (b) TG profiles for ZHTMDBB degraded in nitrogen at a heating rate of 20 °C/min.

Fig. 5.



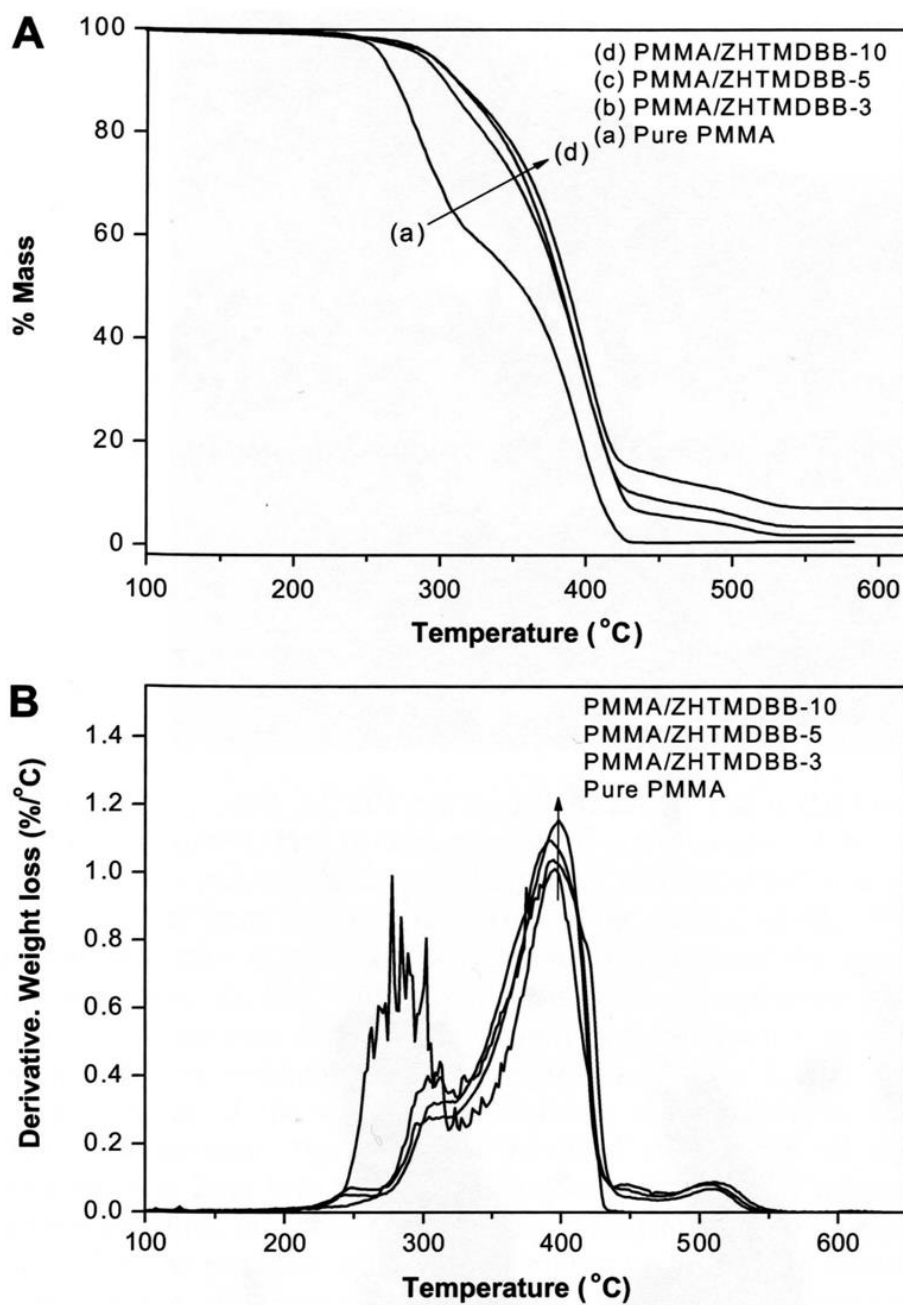
Powder x-ray diffraction data: (a) ZHTMDBB. (b) PMMA/ZHTMDBB-3. (c) PMMA/ZHTMDBB-5. (d) PMMA/ZHTMDBB-10. There is an increase in the basal spacing from 1.45 nm in ZHTMDBB to 1.88 nm in the composites.

Fig. 6.



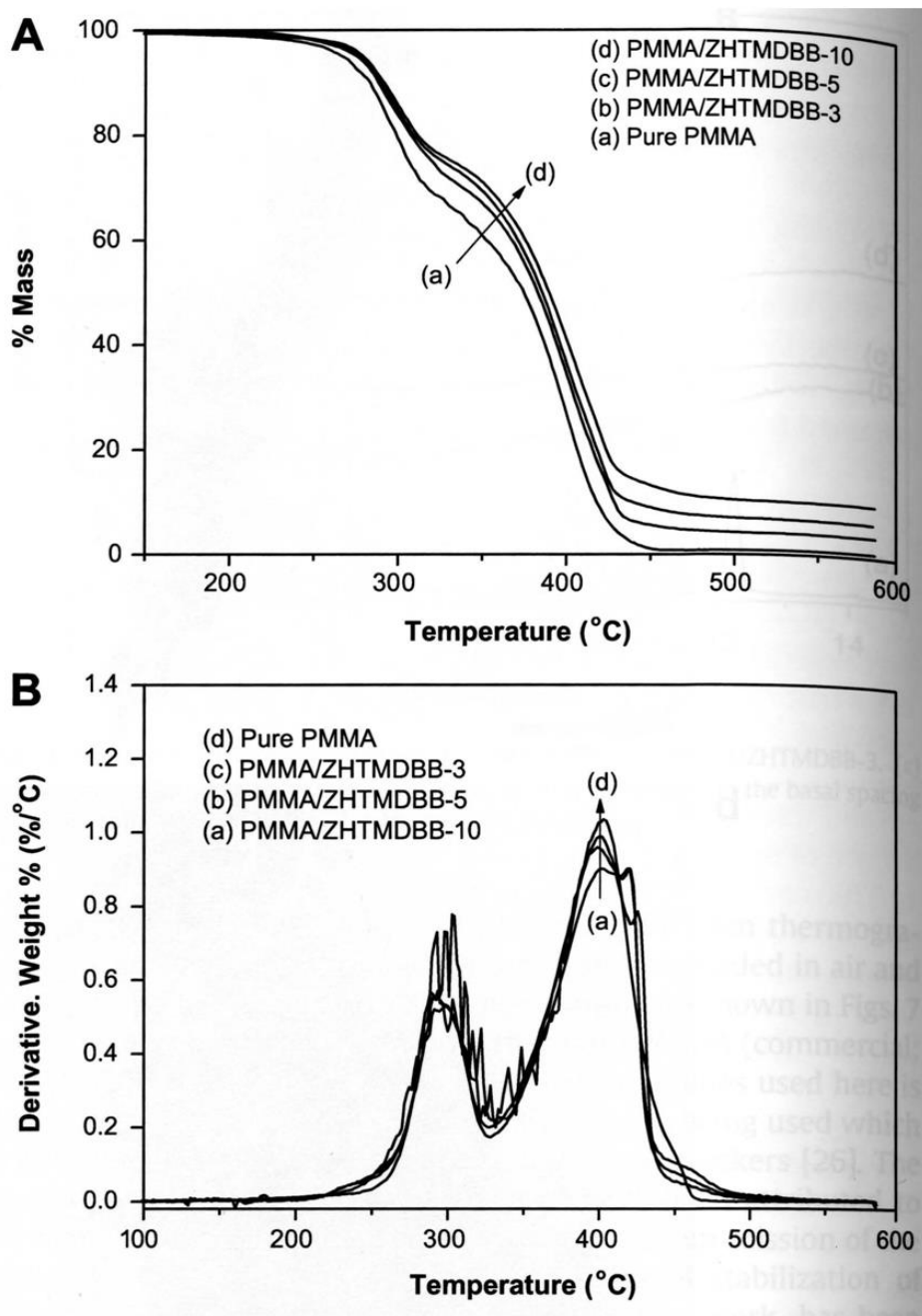
TEM images of polymer composites obtained by melt blending, (a) PMMA/ZHTMDBB-3 and (b) PMMA/ZHTMDBB-10; low magnification (right) and higher magnification (left).

Fig. 7.



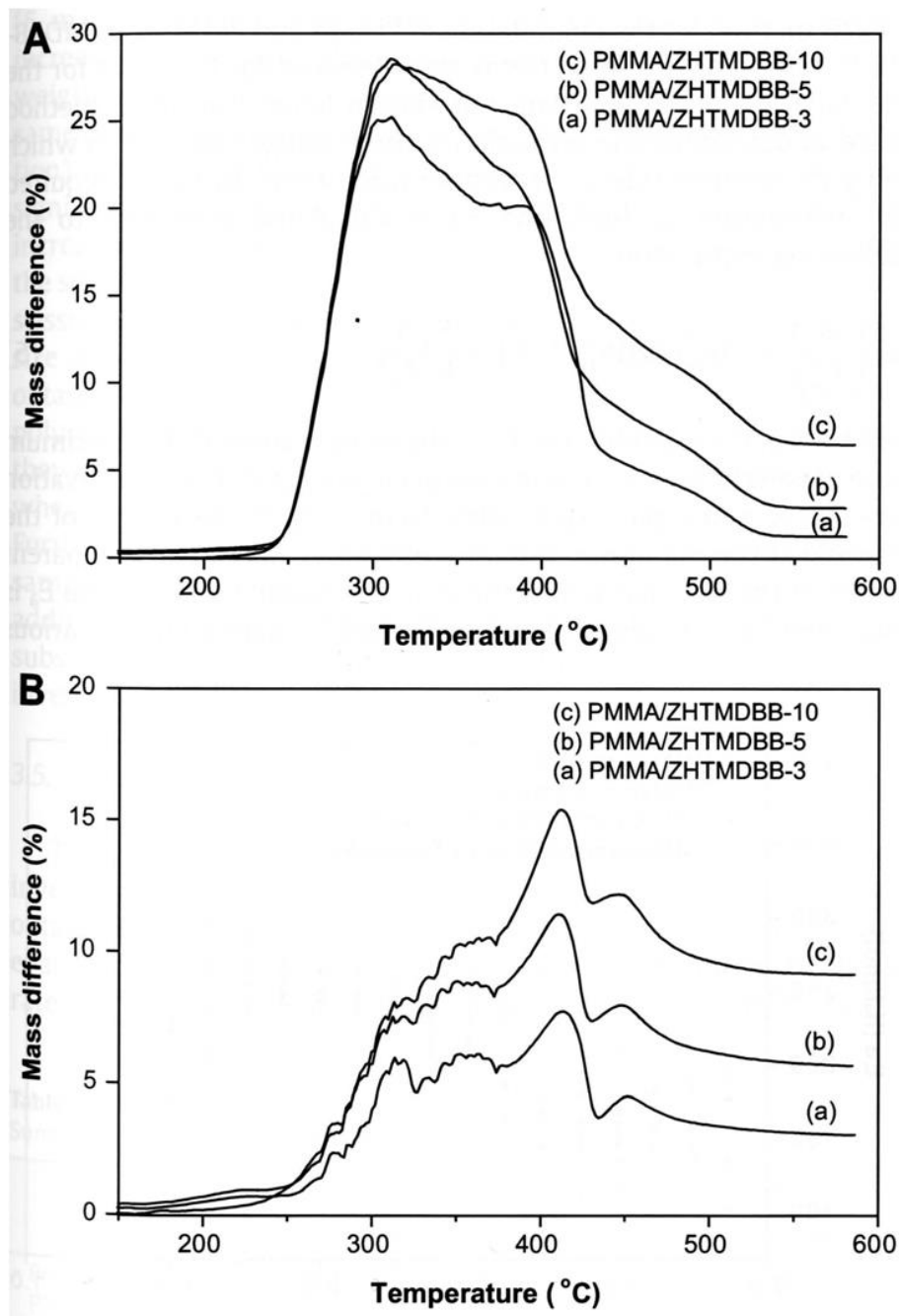
(A). TGA curves for PMMA and composites. (B). DTG curves for PMMA and composites degraded in air at a heating rate of 20 °C/min.

Fig. 8.



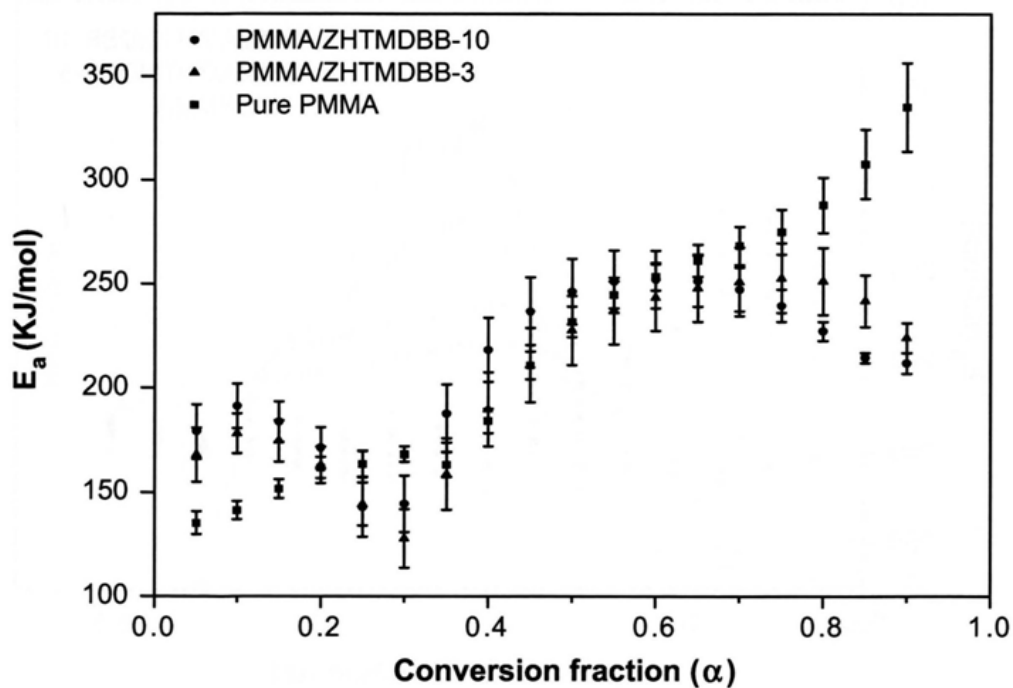
(A). TGA curves for PMMA and composites. (B) DTG curves for PMMA and composites degraded in nitrogen at a heating rate of 20 °C/min.

Fig. 9.



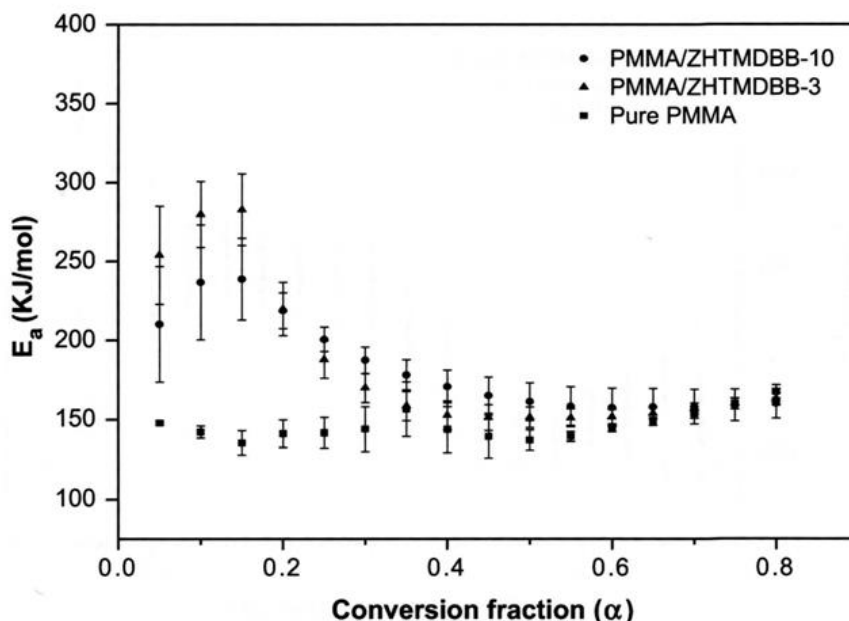
Mass loss difference curves for PMMA composites degradation at a heating rate of 20 °C/min. (A). Degradation in air atmosphere. (B). Degradation in nitrogen atmosphere.

Fig. 10.



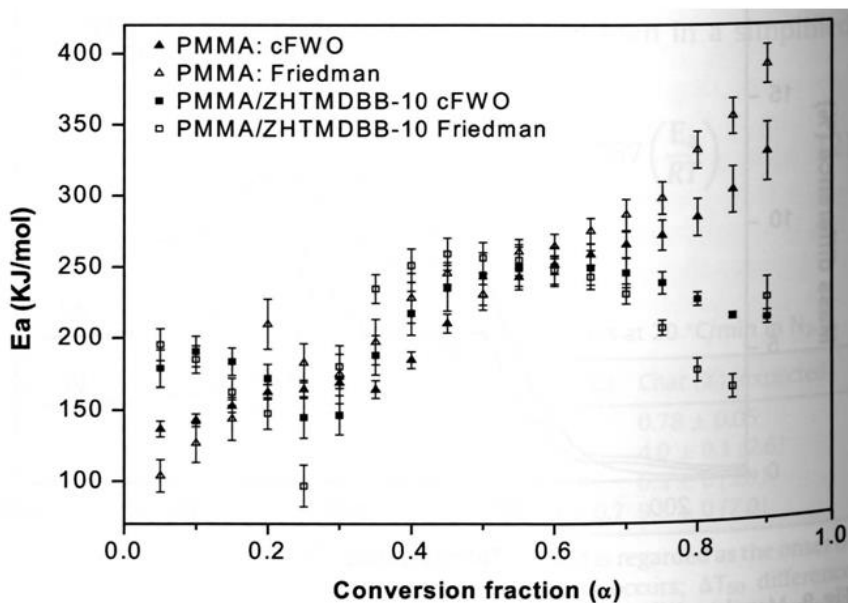
Dependence of E_a on the extent of reaction obtained by cFWO method under nitrogen atmosphere for pure PMMA (closed squares), PMMA/ZHTMDBB -3 (closed triangles) and PMMA/ZHTMDBB -10 (closed circles).

Fig. 11.



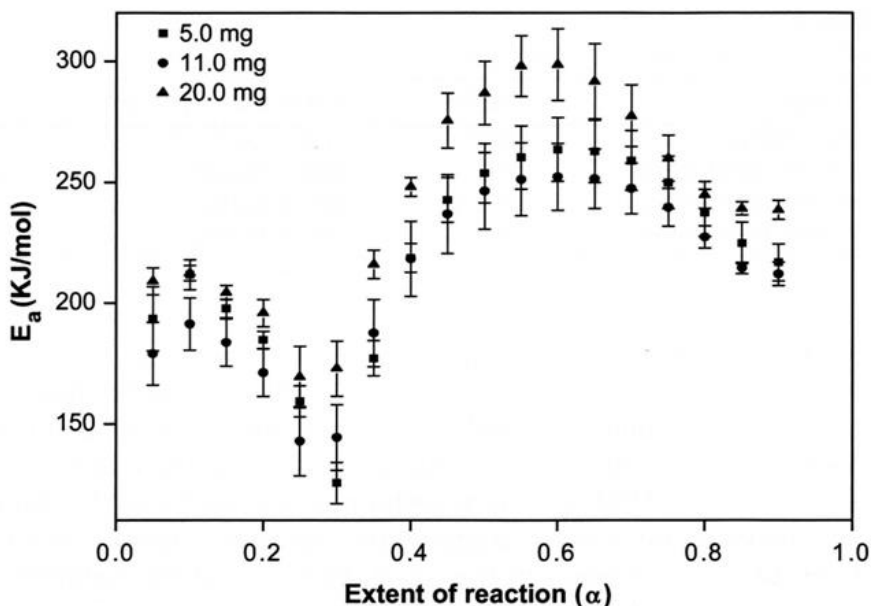
Dependence of E_a on the extent of reaction obtained by cFWO method for degradation under air for pure PMMA (closed squares), PMMA/ZHTMDBB -3 (closed triangles) and PMMA/ZHTMDBB -10 (closed circles).

Fig. 12.



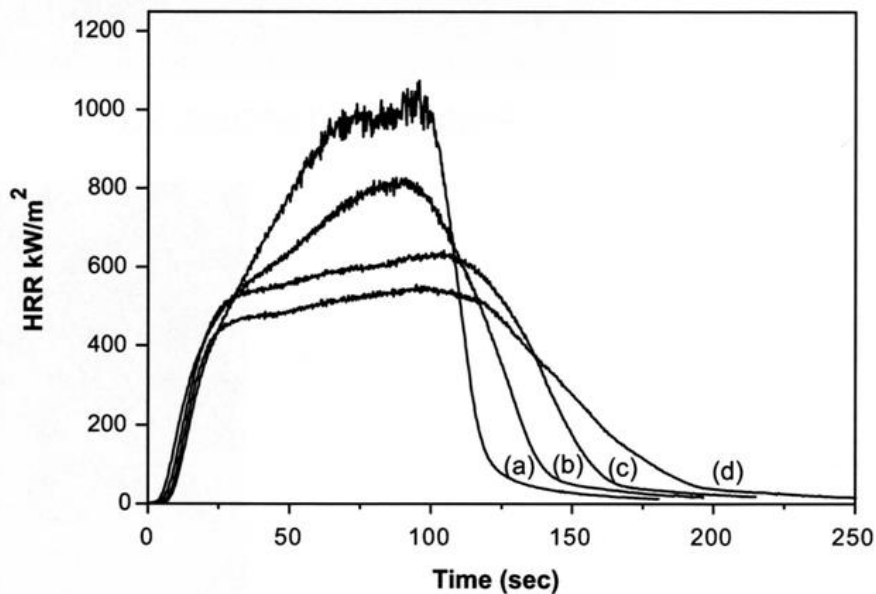
Comparison of corrected Flynn-Wall-Ozawa (cFWO) and Friedman methods for PMMA and PMMA/ZHTMDBB-10 degradation under nitrogen.

Fig. 13.



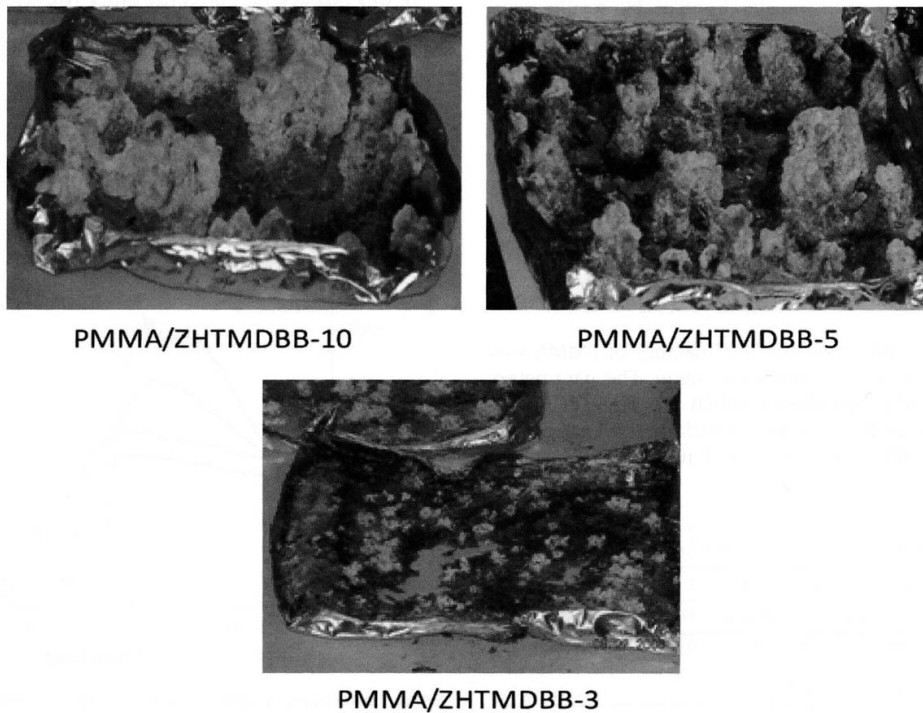
Effect of TGA sample weight on activation energy of PMMA/ZHTMDBB-10 degraded in nitrogen atmosphere.

Fig. 14.



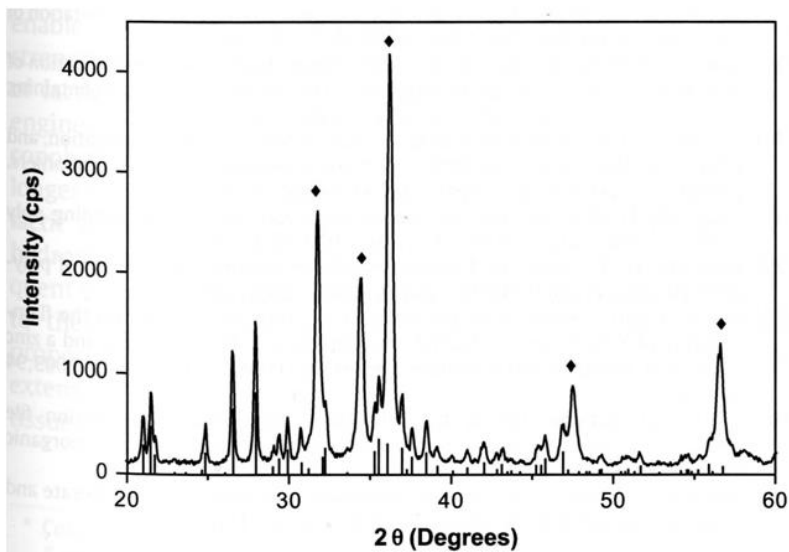
Heat release rate curves for (a) pure PMMA, (b) PMMA/ZHTMDBB-3 (c) PMMA/ZHTMDBB-5 (d) PMMA/ZHTMDBB-10 from cone calorimetry measurements at a heat flux of 50 kW/m².

Fig. 15.



Char of PMMA composites after cone calorimetry test.

Fig. 16.



XRD profile of char residue after cone calorimetry test of PMMA/ZHTMDBB-10 revealing the presence of ZnO [PDF# 36-1451] marked with closed diamonds and stick spectrum provided for ZnB₂O₆ phase [PDF# 27-983].